

NEt ApplicationS of Quantum Computing



D4.5: RO Beta and QCCC Beta

Document Properties

Contract Number	951821
Contractual Deadline	30-06-2023
Dissemination Level	Public
Nature	Report
Editors	Giorgio Silvi, HQS Quantum Simulations Jan Reiner, HQS Quantum Simulations Marko J. Rančić, TotalEnergies Wassil Sennane, TotalEnergies
Authors	Giorgio Silvi, HQS Quantum Simulations Jan Reiner, HQS Quantum Simulations Marko J. Rančić, TotalEnergies Wassil Sennane, TotalEnergies
Reviewers	Thomas Ayrat, Atos Vicente Moret Bonillo, UDC
Date	26-06-2023
Keywords	Quantum computing, benzene, post-Hartree-Fock, VQE, quantum algorithms, quantum chemistry, carbon recapture, measurement optimization, Bayesian statistics, enhanced sampling, n-representability
Status	Under Review
Release	1.0



This project has received funding from the European Union's Horizon 2020 research and innovation programme under Grant Agreement No. 951821



History of Changes

Release	Date	Author, Organisation	Description of Changes
0.1	12-06-2023	Giorgio Silvi and Jan Reiner, HQS Quantum Simulations; Marko J. Rančić and Wassil Sennane, TotalEnergies	Version for Review
0.2	14-06-2023	Giorgio Silvi and Jan Reiner, HQS Quantum Simulations; Marko J. Rančić and Wassil Sennane, TotalEnergies	Implemented changes suggested by Vicente Moret Bonillo
1.0	26-06-2023	Giorgio Silvi and Jan Reiner, HQS Quantum Simulations; Marko J. Rančić and Wassil Sennane, TotalEnergies	Finalized version after internal review



Table of Contents

1	Executive Summary	4
2	Enhanced Sampling	5
2.1	Enhanced Sampling vs. Standard Sampling	5
2.1.1	Standard Sampling	5
2.2	Enhanced Sampling	5
2.2.1	Enhanced-Circuit Choice vs ELF	5
2.2.2	Results	6
2.2.3	Conclusion	6
3	Post-processing noisy quantum computations utilizing N-representability constraints	8
3.1	Theoretical description	8
3.2	Selected Results	9
4	Quantum computing and carbon capture	11
	List of Figures	13
	Bibliography	14



1 Executive Summary

This document gives an overview of the software delivery D4.5 “RO Beta and QCCC Beta”, where RO stands for readout optimization and QCCC stands for quantum computing for carbon capturing. It consists of three main contributions:

Two methods for improving the measurement results of a quantum computation, one based on enhanced sampling using Bayesian statistics and one based on projecting the result to fulfill so-called n-representability constraints which may be violated in a noisy quantum computation. Furthermore, a VQE ansatz investigating the formation of bound states between CO₂ and benzene in the context of utilizing benzene structures to perform CO₂ recapturing.

Consequently, in Chap. 2 we discuss the method for enhanced sampling and show some key results. The software implementation we developed is based on what can be found in literature [1], and we will make the code available in the NEASQC GitHub [2]. Currently, it can be found here:

https://github.com/gsilviHQS/Variationals_algorithms/tree/enhanced_sampling/enhanced_sampling

Next, in Chap. 3 we present briefly the projection method based on n-representability constraints and show selected results. A detailed analysis can be found in our publication on the subject [3]. The software will be made available in the NEASQC GitHub [2] after the review phase. Currently, it can be found here:

https://github.com/gsilviHQS/Variationals_algorithms/tree/enhanced_sampling/n-rep_projection

Finally, in Chap. 4 we give a short discussion of the findings regarding using quantum computing to analyze the formation of a benzene-CO₂ dimer. Again, the code will be made available online in the NEASQC GitHub. It is a continuation of an earlier deliverable [4], where some of the Python script’s dependencies originate from and can also be found. Currently, the program for the benzene-CO₂ dimer calculation is published here:

https://github.com/gsilviHQS/Variationals_algorithms/tree/enhanced_sampling/benzene_CO2



2 Enhanced Sampling

In this chapter, we give an overview of our investigated method of enhanced sampling based on Bayesian statistics. We first motivate the enhanced sampling method compared to standard sampling, continue with a brief description of the Bayesian sampling procedure, and finally show a handful of results from our numerical analysis.

2.1 Enhanced Sampling vs. Standard Sampling

Practical implementation of quantum algorithms often faces significant challenges. One of these challenges is the high demand for measurements in hybrid quantum-classical algorithms such as the Variational Quantum Eigensolver (VQE). In this section we present a new method of sampling in quantum computing that leverages bayesian inference: enhanced sampling [1].

2.1.1 Standard Sampling

Standard sampling in quantum computing, particularly in the context of VQE, involves taking a large number of measurements to estimate the expectation value of a Hamiltonian. This process can be computationally expensive and time-consuming, especially for complex problems. The accuracy of the results depends on the number of measurements taken, with more measurements generally leading to more accurate results. However, the high demand for measurements can be a significant barrier for many practical applications.

2.2 Enhanced Sampling

The enhanced sampling method proposed in the paper "Minimizing estimation runtime on noisy quantum computers" [1] is a technique that maximizes the statistical power of noisy quantum devices. This method is inspired by quantum-enhanced metrology, phase estimation, and the more recent "alpha-VQE" and aims to improve the efficiency of quantum amplitude estimation.

In standard sampling, as used in Variational Quantum Eigensolver (VQE), the estimation process is insensitive to small deviations in the expectation value, leading to low information gain from measurement outcomes. This results in a high runtime cost for for interesting practical problems.

Enhanced sampling addresses this issue by engineering likelihood functions that increase the rate of information gain, thereby reducing the runtime of amplitude estimation. The method involves preparing an ansatz state, applying an operator, adding a phase shift about the ansatz state, and then measuring the operator. The phase shift can be achieved by performing the inverse of the ansatz circuit, then a phase shift about the initial state, and then re-applying the ansatz circuit. An example with 1 layer is shown in Fig.1

The likelihood function in enhanced sampling is a degree-3 Chebyshev polynomial in the expectation value, referred to as a Chebyshev likelihood function (CLF). This is in contrast to standard sampling, where the likelihood function is a degree-1 polynomial. The higher degree polynomial in enhanced sampling leads to a higher rate of information gain, which reduces the runtime of the estimation process.

2.2.1 Enhanced-Circuit Choice vs ELF

In the paper "Minimizing estimation runtime on noisy quantum computers" [1], the Engineered Likelihood Function (ELF) is used to estimate the parameters of a quantum circuit. The ELF maps the parameters of the quantum circuit to a likelihood value, which measures how well the circuit fits the data. It is constructed by defining a prior distribution over the parameters, and then using Bayes' rule to compute the posterior distribution given the data. The likelihood function is then defined as the marginal distribution of the data given the parameters. The ELF is used to perform maximum likelihood estimation of the parameters, which involves finding the parameters that maximize the likelihood function. This is done using a classical optimization algorithm, such as gradient descent.

In our work [2], we have chosen to implement an alternative approach where, for a given ansatz and some pre-sampling, the algorithm selects between two enhanced-circuit with different number of layers, instead of using the Engineered Likelihood Function (ELF). This method involves selecting the enhanced circuit with the highest Fisher

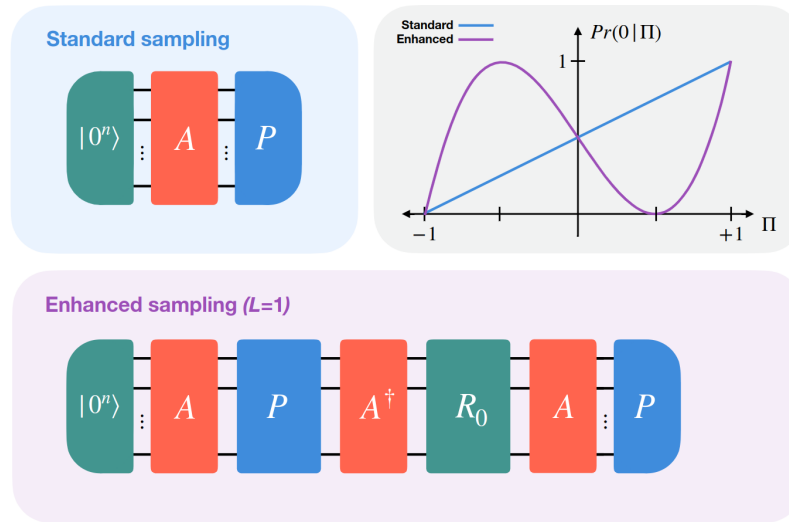


Figure 1: Circuit for standard sampling vs enhanced sampling. Source [1].

information to be used for sampling. Fisher information is a measure of the amount of information that an observable random variable carries about an unknown parameter, and maximizing it can lead to more efficient sampling.

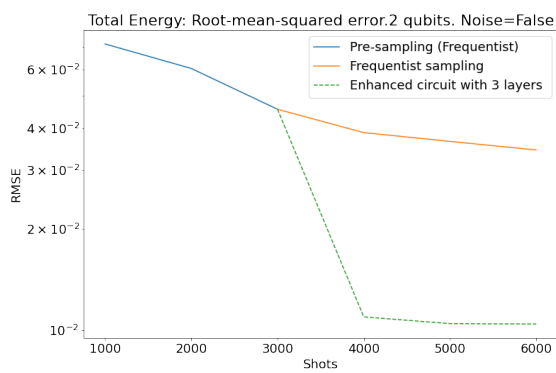
By selecting the circuit with the highest Fisher information, we aim to maximize the information gain from each measurement, thereby reducing the total number of measurements needed. This approach is more practical for our purposes than implementing the ELF, as it does not require the time-consuming adaptive scheme to be applied at every shot.

2.2.2 Results

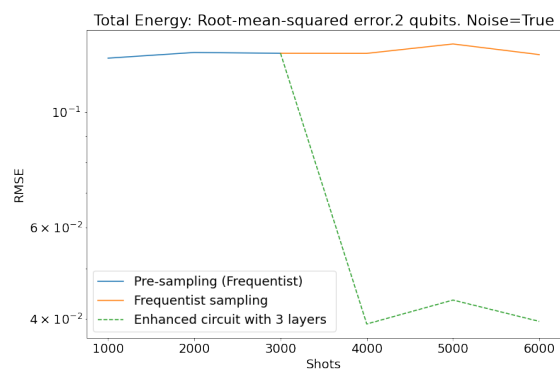
In our repository, we offer a demonstrative notebook that showcases the capabilities of the algorithm. Specifically, given a Hamiltonian and an ansatz, we evaluate the root mean square error of the measured energy relative to the exact energy. As illustrated in Fig.2, following an initial shared presampling phase (standard), we compare the performance of the enhanced sampling technique to that of standard sampling as additional measurements are conducted in both scenarios. In a noiseless environment, it is evident that the enhanced sampling technique outperforms standard sampling. However, this improvement is accompanied by a rise in complexity and, more significantly, an increase in circuit depth. The latter is particularly disadvantageous in noisy environments such as those experienced by Near-Term Intermediate-Scale Quantum (NISQ) devices. This drawback is evident in the case of the noisy 3-qubit system depicted in Fig.2d. Here, the performance of enhanced sampling deteriorates to a point below that of standard sampling.

2.2.3 Conclusion

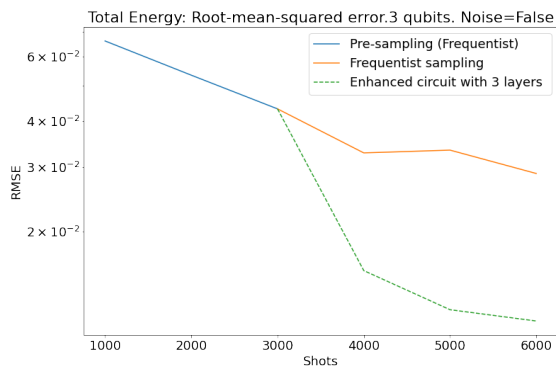
While the ELF formalism offers a promising method for enhancing the power of sampling on quantum devices, its practical implementation can be challenging due to the time required for the adaptive scheme. The two enhanced-circuit choice offers a practical alternative that can reduce the number of measurements and runtime compared to standard sampling, making it a promising approach for the implementation of quantum algorithms in practical applications.



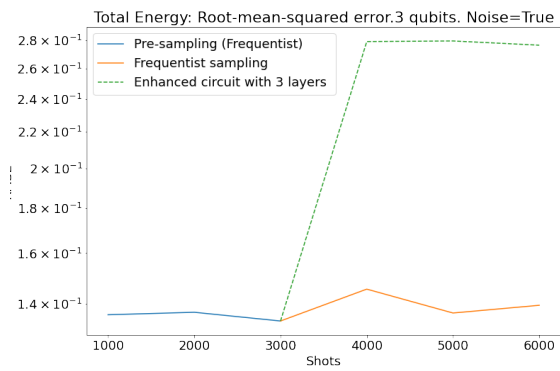
(a) 5 Runs on a 2-qubit EfficientSU2 ansatz on a noiseless simulator.



(b) 5 Runs on a 2-qubit EfficientSU2 ansatz on a noisy simulator.



(c) 5 Runs on a 3-qubit EfficientSU2 ansatz on a noiseless simulator.



(d) 5 Runs on a 3-qubit EfficientSU2 ansatz on a noisy simulator.

Figure 2: Root mean square errors for various experimental setups and configurations.

3 Post-processing noisy quantum computations utilizing N-representability constraints

In this chapter, we consider a method for improving the results of a noisy quantum computation, e.g., obtained from a NISQ device. We will describe here briefly how the method works in the following theory subsection and show some selected results in the subsequent subsection. A thorough analysis of the approach, including a detailed explanation of the method and the motivation behind it, as well extensive numerical data and a discussion of its caveats are given in our publication on this subject [3]:

Tomislav Piskor, Florian G. Eich, Michael Marthaler, Frank K. Wilhelm, and Jan-Michael Reiner, *Post-processing noisy quantum computations utilizing N-representability constraints*, arXiv:2304.13401 [quant-ph] (2023), <https://arxiv.org/abs/2304.13401>

3.1 Theoretical description

The internal energy is given by the expectation value of the Hamiltonian,

$$\langle H \rangle = E_0 + \sum_{ij} t_{ij} ({}^1D_{ij}) + \sum_{ijkl} V_{ijkl} ({}^2D_{ijkl}), \quad (3.1)$$

with the annihilation (creation) operators $c_i^{(\dagger)}$ of an electron in orbital i , the energy offset E_0 , the one- and two-electron integrals t_{ij} and V_{ijkl} , as well as the one-particle RDM,

$${}^1D_{ij} = \langle c_i^\dagger c_j \rangle, \quad (3.2)$$

and the two-particle RDM

$${}^2D_{ijkl} = \langle c_i^\dagger c_j^\dagger c_l c_k \rangle. \quad (3.3)$$

If 1D and 2D of the ground state are obtained from a quantum computation on a NISQ device, they are obscured by decoherence and shot noise. We assume, that the dominating noise source is decoherence, and in this case, the calculated energy would be higher than the actual ground state energy.

One can mitigate this error and the statistical variance from shot noise by imposing constraints that the RDMs need to fulfill:

From the anti-commutation relations of the fermionic operators, one can derive that they are Hermitian and obey a certain set of anti-symmetry relations. These constraints are usually fulfilled in a quantum computation by simply calculating only a minimal necessary set of matrix elements and reconstructing the rest through the Hermiticity and anti-symmetry constraints.

Less trivial are the constraints that the RDMs need to be positive semi-definite and the trace is given by the particle number n :

$$\begin{aligned} \text{tr}({}^1D) &= n, \\ \text{tr}({}^2D) &= n(n-1). \end{aligned}$$

We impose these by projecting; we find the RDM that fulfills these conditions and is, in some norm, closest to the RDM calculated on the quantum computer.

Furthermore, one can transform the one- and two-particle RDMs into the hole and particle-hole sector. This means we can transform to the one- and two-hole RDMs,

$${}^1D_{ij} = \langle c_i c_j^\dagger \rangle, \quad (3.4)$$

$${}^2D_{ijkl} = \langle c_i c_j c_l^\dagger c_k^\dagger \rangle, \quad (3.5)$$

and the particle-hole RDM,

$${}^2G_{ijkl} = \langle c_i^\dagger c_j c_l^\dagger c_k \rangle. \quad (3.6)$$

In these sectors, the same constraints hold (where the trace now depends not only on the number of electrons in the system, but also the number of holes). Instead of measuring, projecting, and calculating the energy in the particle sector, one can, after measurement, transform into a different sector, project there, transform back to the particle RDMs and calculate the energy.

We perform the projection of the measured RDMs in all three sectors, and return the energetically best of these results, as we assume the noise to be dominated by decoherence.

Again, more detailed information and reasoning can be found in our paper [3].

3.2 Selected Results

To showcase the performance of the method, we give here examples of a ground state calculation of H_2 under the influence of damping noise in Fig. 3, and under the influence of damping noise and shot noise in Fig. 4. For damping noise only we look at the energy difference of the calculation to the actual ground state energy, as well as the final state fidelity. When including shot noise, we looked at the energy difference to the ground state and the measurement variance.

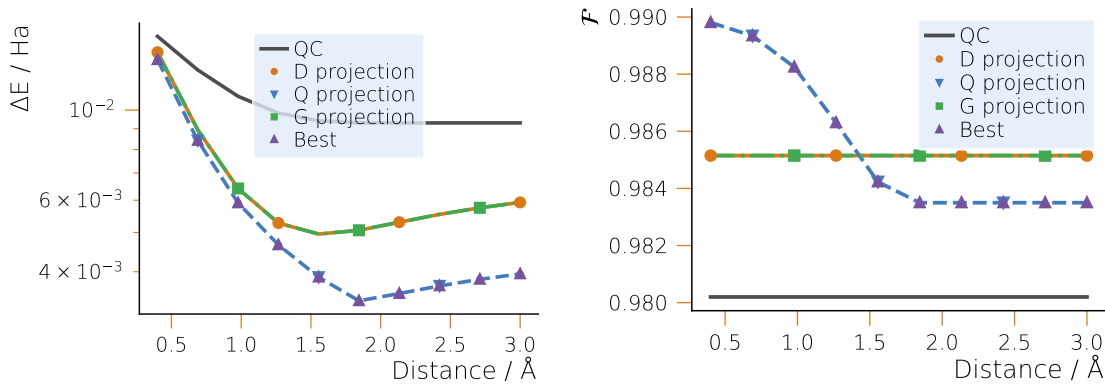


Figure 3: Energy difference to the ground state and fidelity of the final state towards the exact ground state for H_2 ; directly from the quantum calculation (QC), the three individual projection in the particle, hole, or particle-hole sector (D, Q, or G) and the energetically best result (Best).

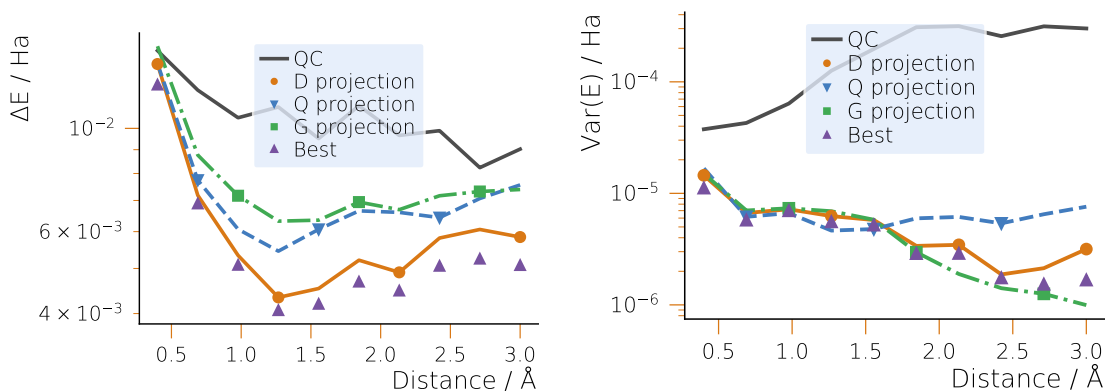


Figure 4: Energy difference to the ground state and measurement variance for H_2 ; directly from the quantum calculation (QC), the three individual projection in the particle, hole, or particle-hole sector (D, Q, or G) and the energetically best result (Best).



In Fig. 3, note the improvement of the energy difference of almost an order of magnitude. Note also the general improvement in fidelity, but that the energetically best result does not guarantee the best fidelity.

In Fig. 4, we should mention that *Best* is strictly lower than other projections in this case, as here we average over 100 repetitions of the same measurement with different shot noise, to obtain a variance, and in each repetition different projections might lead to the energetically best result. The plot shows significant improvement of the energy difference, but also – and arguably more importantly – the reduction of the measurement variance up to two orders of magnitude. Note also that there is general reduction in the variance, but that the energetically best result does not guarantee the smallest variance.

Once more, for a detailed numerical analysis see our manuscript [3].

4 Quantum computing and carbon capture

NISQ computing algorithms, including the Variational Quantum Eigensolver (VQE), play a significant role in the current era of quantum computing. NISQ devices are characterized by their intermediate scale, consisting of tens to hundreds of qubits with a limited coherence time. Despite the inherent noise and imperfections in these quantum systems, NISQ algorithms offer promising solutions to tackle complex computational problems. VQE, in particular, is a hybrid quantum-classical algorithm that addresses problems in quantum chemistry and optimization. By leveraging quantum circuits and classical optimization techniques, VQE aims to find the ground state energy of a given molecular system. It does so by constructing a parameterized quantum circuit, known as an ansatz, and iteratively adjusting the parameters to minimize the energy expectation value. Although VQE is susceptible to noise and errors, it can still provide valuable insights into molecular properties and help optimize chemical processes in areas like drug discovery and materials science.

The VQE algorithm's strength lies in its ability to utilize limited quantum resources efficiently while mitigating the effects of noise and errors. This approach is particularly suitable for NISQ devices, where achieving fault-tolerant quantum computing is a significant challenge. VQE's adaptability makes it a promising candidate for near-term quantum applications, as it can be executed on current quantum hardware with a reasonable number of qubits. Moreover, VQE's hybrid nature allows it to take advantage of classical optimization algorithms, making it more robust against the inherent noise and inaccuracies of NISQ devices. Researchers continue to explore various enhancements to VQE, such as improved ansatz construction techniques, noise mitigation strategies, and error correction methods, to improve the algorithm's performance and broaden its applicability. As the field of NISQ quantum computing progresses, algorithms like VQE are expected to play a vital role in advancing quantum technologies and unlocking their potential in solving real-world problems.

In this deliverable we model the energy of the benzene- CO_2 dimer as a function of distance (see Fig. 5) to model a potential procedure using benzene structures to recapture CO_2 . We compare a hardware efficient ansatz to qUCCSD and exact diagonalization (see Fig. 6). The dimer doesn't have any clear minimum as a function of distance for the mean field HF solution, qUCCSD or exact diagonalization. The only method which gives a minimum is the hardware efficient ansatz but this is quite likely due to the low expressibility of this ansatz.

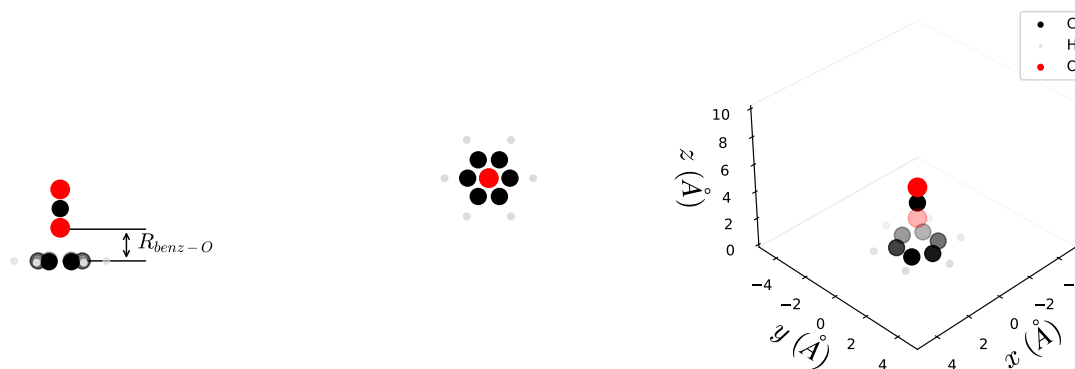


Figure 5: Benzene- CO_2 dimer distance displayed.

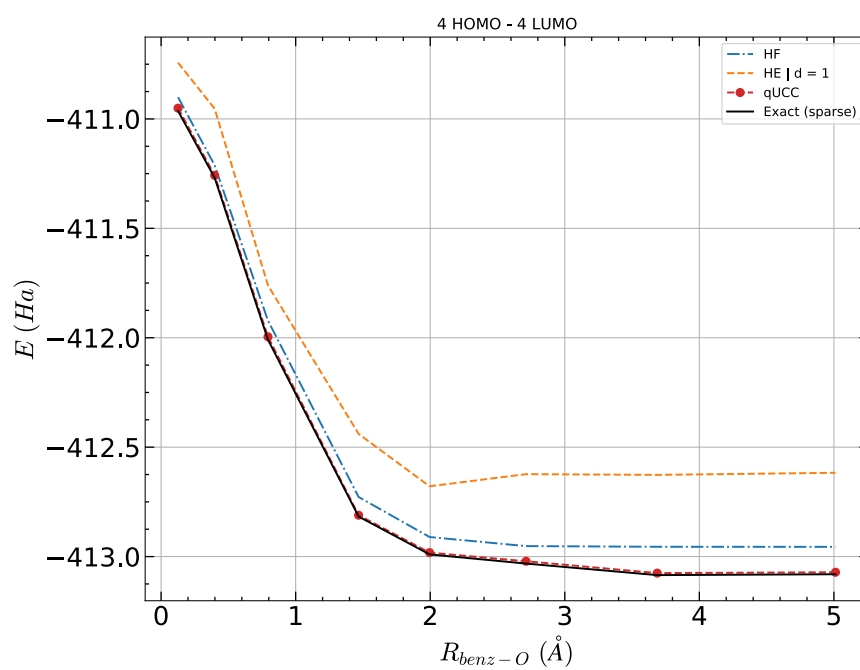


Figure 6: The energy of the benzene-CO₂ dimer as a function of distance.



List of Figures

Figure 1: Circuit for standard sampling vs enhanced sampling. Source [1].	6
Figure 2: Root mean square errors for various experimental setups and configurations.	7
Figure 3: Energy difference to the ground state and fidelity of the final state towards the exact ground state for H_2 ; directly from the quantum calculation (QC), the three individual projection in the particle, hole, or particle-hole sector (D, Q, or G) and the energetically best result (Best).	9
Figure 4: Energy difference to the ground state and measurement variance for H_2 ; directly from the quantum calculation (QC), the three individual projection in the particle, hole, or particle-hole sector (D, Q, or G) and the energetically best result (Best).	9
Figure 5: Benzene- CO_2 dimer distance displayed.	11
Figure 6: The energy of the benzene- CO_2 dimer as a function of distance.	12



Bibliography

- [1] G. Wang, D. E. Koh, P. D. Johnson, and Y. Cao, *Minimizing estimation runtime on noisy quantum computers*, PRX Quantum **2**, 010346 (2021)
- [2] NEASQC, Variational Algorithms, GitHub repository, https://github.com/NEASQC/Variationals_algorithms
- [3] T. Piskor, F. G. Eich, M. Marthaler, F. K. Wilhelm, and J.-M. Reiner, *Post-processing noisy quantum computations utilizing N-representability constraints*, arXiv:2304.13401 [quant-ph] (2023), <https://arxiv.org/abs/2304.13401>
- [4] NEASQC, D4.2, GitHub repository, <https://github.com/NEASQC/D4.2>